Article

Not peer-reviewed version

Characterization of BSK Homologs in *Brassica rapa* subsp. *chinensis* and Their Transcriptional and Physiological Alterations Under Thermal Stress

Lijuan Yang , Jiahui Wang , Pan Yuan , Xiang Li , Xiaofeng Li * , Bo Zhu *

Posted Date: 9 April 2026

doi: 10.20944/preprints202604.0627.v1

Keywords: *Brassica rapa* subsp. *chinensis*; BR-signaling kinase genes; high-temperature stress; brassinosteroid hormones; expression dynamics; stress physiology

 doi:10.20944/preprints202604.0627.v1

Article

Characterization of BSK Homologs in *Brassica rapa* subsp. *chinensis* and Their Transcriptional and Physiological Alterations Under Thermal Stress

Lijuan Yang [1], Jiahui Wang [1], Pan Yuan [1], Xiang Li [1], Xiaofeng Li [2,*] and Bo Zhu [1,*]

[1] Key Laboratory for the Conservation and Utilization of Important Biological Resources, College of Life Sciences, Anhui Normal University, Wuhu, 241000, Anhui Province, China

[2] Shanghai Key Laboratory of Protected Horticultural Technology, Horticultural Research Institute, Shanghai Academy of Agricultural Sciences, 201403 Shanghai, China

* Correspondence: lixiaofeng@saas.sh.cn (X.L.); zhubo@ahnu.edu.cn (B.Z.)

Abstract

Plant steroid hormones, namely brassinosteroids (BRs), govern growth and resilience to environmental stress, yet little is known about how BR-signaling kinases (BSKs) operate in non-model horticultural species. Here, we carried out a whole-genome interrogation of the BSK family in *Brassica rapa* subsp. *chinensis* and examined its potential involvement in high-temperature stress responses. The search yielded 20 BcBSK members, each featuring a conserved kinase domain at the N-terminus and TPR repeats at the C-terminus. Phylogenetic reconstruction assigned them to separate subgroups, while collinearity assessment detected 16 duplicated gene pairs evolving under strong selection constraints. Upstream regulatory sequences harbored numerous cis-motifs linked to hormonal signals and stress perception. Interactome modeling pinpointed BcBSK2, BcBSK5, BcBSK14, and BcBSK18 as hub components. RNA-seq analysis under elevated temperature (38℃) uncovered distinct expression behaviors between cultivars: in the susceptible line "Aijiaohuang", BcBSK1 and BcBSK2 transcripts increased sharply, whereas the resistant line "SHI" exhibited little fluctuation. Quantitative PCR results aligned with the RNA-seq findings. Exogenous application of 0.5 mg·L^{-1} BR improved the activities of catalase, peroxidase, and superoxide dismutase, boosted proline levels, lowered malondialdehyde content, and preserved chlorophyll and carotenoid concentrations under heat exposure. Taken together, these data imply that BcBSK family members contribute to BR-facilitated heat adaptation by orchestrating changes at both transcript and metabolite levels, thus laying a groundwork for genetic enhancement of thermotolerance in this vegetable species.

Keywords: *Brassica rapa* subsp. *chinensis*; BR-signaling kinase genes; high-temperature stress; brassinosteroid hormones; expression dynamics; stress physiology

1. Introduction

Non-heading Chinese cabbage (NHCC, *Brassica rapa* subsp. *chinensis*) is an important leafy vegetable widely cultivated in China. It is characterized by a short growth cycle and high yield; however, it is highly sensitive to temperature fluctuations. Exposure to high temperatures often results in growth inhibition and deterioration of leaf quality, ultimately reducing yield and marketability [1,2]. Therefore, understanding the molecular mechanisms underlying heat stress responses in NHCC is essential for the development of heat-tolerant cultivars.

Phytohormone signaling pathways play central roles in plant adaptation to high temperature and other abiotic stresses. Among these, brassinosteroids (BRs), a class of plant steroidal hormones, are key regulators involved in diverse developmental processes and stress responses [3–5]. BR signaling is initiated when the plasma membrane receptor BRI1 perceives BR ligands and subsequently forms a complex with the co-receptor BAK1, triggering phosphorylation events. The

 doi:10.20944/preprints202604.0627.v1

signal is then transduced through a cascade of cytoplasmic components, ultimately regulating the activity of BZR/BES transcription factors and controlling downstream gene expression [6–9]. Within this pathway, BR-signaling kinases (BSKs), as direct substrates of BRI1, function at an early stage of signal transduction, linking membrane receptors to downstream signaling networks and acting as critical regulatory hubs [10,11].

BSK proteins belong to the RLCK-XII subfamily of receptor-like cytoplasmic kinases and typically contain an N-terminal protein kinase catalytic domain and C-terminal tetratricopeptide repeat (TPR) motifs [3,12–14]. This modular structure enables BSKs to integrate kinase activity with protein–protein interactions during signal transduction. Evolutionary analyses have shown that the BSK gene family exhibits lineage-specific diversification in plants. Distinct subgroups differ in species composition, with some clades enriched in monocots or dicots, whereas complete BSK homologs are absent in lower plants [3,15].

Functionally, BSK family members display considerable diversity. In *Arabidopsis thaliana*, twelve BSK proteins participate not only in BR signaling but also in root development, low-nitrogen responses, and immune regulation [16–18]. For example, BSK1 directly interacts with the immune receptor FLS2 and is involved in plant immune responses [19–21], whereas BSK5 participates in salt stress responses and abscisic acid (ABA) signaling [22,23]. In rice, OsBSK1-2 positively regulate immune resistance [24,25], and OsBSK2 controls grain size independently of BR signaling [26]. These findings highlight the multifunctional roles of BSK proteins in coordinating plant growth, development, and stress adaptation.

Despite these advances, a systematic understanding of BSK functions under specific stress conditions remains limited. In particular, although exogenous BR application has been shown to enhance plant thermotolerance [27–30], the roles of key components in BR signal transduction during heat stress are still unclear. As early components of the BR signaling pathway, whether BSK family members exhibit functional differentiation in heat stress responses remains to be elucidated. Moreover, most existing studies have focused on model plants, and evidence from vegetable crops such as NHCC is still scarce.

In this study, the BSK gene family in NHCC was identified at the whole-genome level. By integrating transcriptomic and physiological data, the expression patterns of *BSK* genes under heat stress were analyzed. Furthermore, gene family characterization, expression profiling, and physiological responses were combined to compare functional differences among individual members and to explore their associations with physiological changes induced by exogenous BR treatment. This study provides new insights into the functional divergence of BSK family members and offers a theoretical basis for elucidating the molecular mechanisms of BR-mediated heat stress responses, thereby contributing to the improvement of heat tolerance in NHCC.

2. Materials and Methods

2.1. Identification and Physicochemical Characterization of the BcBSK Gene Family

To identify members of the BcBSK gene family in NHCC, a combined approach integrating sequence homology searches and domain-based screening was applied. First, twelve reported AtBSK protein sequences from *Arabidopsis thaliana* were used as queries [3], and a local BLASTP search was performed against the NHCC protein database with an E-value threshold of 1e−100 to obtain candidate homologs. Subsequently, hidden Markov models (HMMs) corresponding to PF07714 and PF25575 from the Pfam database were employed to scan the proteome using HMMER to identify additional candidates.

The results from BLASTP and HMMER were integrated, and candidate sequences were subjected to conserved domain validation. Domain annotation was performed using the Conserved Domain Database (CDD) and InterProScan, and only sequences confirmed by both methods to contain complete characteristic domains of the BSK family were retained as final members.

 doi:10.20944/preprints202604.0627.v1

Physicochemical properties, including amino acid length, molecular weight (MW), and theoretical isoelectric point (pI), were predicted using the ExPASy ProtParam tool. Subcellular localization was predicted using DeepLoc 2.1.

2.2. Phylogenetic Analysis of the BcBSK Gene Family

Multiple sequence alignment of BSK proteins was conducted using BioEdit. The aligned sequences were then used to construct a phylogenetic tree using IQ-TREE (v2.4.0) based on the maximum likelihood (ML) method.

The optimal substitution model was selected using ModelFinder according to the Bayesian Information Criterion (BIC), with Q. plant+G4 identified as the best-fit model. Branch support was assessed using the ultrafast bootstrap method with 1000 replicates. The resulting tree was visualized and edited using iTOL (Interactive Tree Of Life).

2.3. Chromosomal Localization, Synteny, and Ka/Ks Analysis

Chromosomal locations of *BcBSK* genes were determined using TBtools [31]. Intraspecies synteny analysis was performed using the "One Step MCScanX" function in TBtools to identify collinear gene pairs and duplicated regions.

To evaluate selection pressure, nonsynonymous substitution rates (Ka), synonymous substitution rates (Ks), and their ratios (Ka/Ks) were calculated using KaKs_Calculator 3.0 [32]. A Ka/Ks ratio > 1 indicates positive selection, = 1 indicates neutral evolution, and < 1 indicates purifying selection [33].

2.4. Gene Structure and Conserved Domain Analysis

Gene structures and conserved protein features were analyzed based on genome annotation files and corresponding protein sequences of NHCC. Exon–intron structures were visualized using TBtools.

Conserved domains were annotated using InterProScan and the CDD database. Conserved motifs were identified using MEME Suite, with parameters set to a maximum of eight motifs and motif lengths ranging from 6 to 50 amino acids. Phylogenetic relationships, gene structures, motif composition, and domain organization were integrated and visualized using TBtools.

2.5. Cis-Acting Element Analysis

Promoter sequences (2000 bp upstream of the translation start site, ATG) were extracted for each *BcBSK* gene. Cis-acting regulatory elements were identified using the PlantCARE database. The results were further processed and visualized using TBtools.

2.6. Protein–Protein Interaction Network Analysis

Protein–protein interaction (PPI) networks were constructed using the STRING database (version 11.0). Protein sequences were mapped based on homology using the Chinese cabbage reference genome under default parameters [34]. The interaction data were visualized and analyzed using Cytoscape (version 3.8.0) to evaluate network topology [35].

2.7. Transcriptome Data and Expression Analysis

Expression profiles of *BcBSK* genes under heat stress were analyzed using RNA-seq data obtained from the NCBI BioProject database (PRJNA1030162). The dataset included samples from the heat-sensitive cultivar "Aijiaohuang" and the heat-tolerant cultivar "SHI" treated at 38 °C for 0, 6, and 24 h.

Gene expression levels were quantified as FPKM (Fragments Per Kilobase of transcript per Million mapped reads). Differentially expressed genes were identified using the thresholds $|\log_2$(fold

 doi:10.20944/preprints202604.0627.v1

change)| ≥ 1 and FDR-adjusted $p < 0.05$. The normalized expression data were visualized as heatmaps using TBtools.

2.8. qRT–PCR Validation

Gene-specific primers were designed using Primer 5.0, and the sequences are listed in Supplementary Table S1. First-strand cDNA was synthesized using the RTase III Primer Flexible All-in-One Mix kit, including genomic DNA removal.

qRT–PCR was performed using a SYBR Green Premix kit in a total reaction volume of 20 μL, containing 1 μL cDNA template, 10 μL Premix, 0.4 μL of each primer (0.2 μM), and 8.2 μL ddH_2O. Each sample included three biological replicates.

The amplification conditions were as follows: 95 °C for 30 s, followed by 40 cycles of 95 °C for 10 s and 60 °C for 30 s. Relative expression levels were calculated using the $2^{-\Delta\Delta Ct}$ method.

2.9. Plant Materials, Treatments, and Physiological Measurements

The heat-sensitive cultivar "Aijiaohuang" and the heat-tolerant cultivar "SHI" of NHCC were used in this study. Seeds were provided by the Horticultural Research Institute of the Shanghai Academy of Agricultural Sciences. Heat tolerance identification and transcriptomic data for these materials were derived from previous studies conducted by our research group[36].

Seeds were germinated in a growth chamber under controlled conditions (25/20 °C day/night, 16 h light/8 h dark, light intensity 12,000 lx). At the 4-5 leaf stage, plants were treated by foliar spraying with deionized water (control), 0.10, 0.50, or 1.00 mg·L^{-1} BR once daily for three consecutive days.

Heat stress was applied on the fourth day (15:00) by transferring plants to 40/30 °C (day/night) conditions with a 12 h photoperiod. Samples were collected at 0, 3, 6, and 9 days after treatment.

Physiological parameters were measured following standard methods [37]. Proline content was determined using the acid ninhydrin method; SOD activity by the nitroblue tetrazolium method; POD activity using the guaiacol method; MDA content using the thiobarbituric acid method; chlorophyll content by ethanol extraction; and CAT activity spectrophotometrically. All measurements were performed on a fresh weight basis with three replicates.

It should be noted that the transcriptomic analysis and physiological experiments were conducted under different heat stress regimes. The RNA-seq data (38 °C, 0-24 h) were used to capture early transcriptional responses, whereas the physiological experiments (40/30 °C, up to 9 d) were designed to evaluate longer-term stress adaptation and the effects of exogenous BR treatment. These complementary approaches enable a comprehensive understanding of both early molecular responses and subsequent physiological changes under heat stress.

2.10. Statistical Analysis

Data were processed using Microsoft Office 2019. Statistical analyses were conducted using SPSS 27, and figures were generated using GraphPad Prism 10.2. Results.

3. Results

3.1. Genome-Wide Identification and Physicochemical Characterization of BcBSK Proteins in NHCC

A total of 20 *BcBSK* genes were identified in the NHCC genome (Table 1) and were designated *BcBSK1* to *BcBSK20*. The encoded proteins ranged from 465 to 511 amino acids (aa) in length, with molecular weights (MW) of 52.29–57.92 kDa and theoretical isoelectric points (pI) of 5.17–8.74.

The instability index ranged from 34.87 to 50.92, with most proteins exceeding 40. The grand average of hydropathicity (GRAVY) values ranged from − 0.543 to − 0.316. Subcellular localization prediction indicated that all BcBSK proteins were localized to the plasma membrane. The aliphatic

 doi:10.20944/preprints202604.0627.v1

index ranged from 67.42 to 82.94, with BcBSK2, BcBSK10, BcBSK12, BcBSK17, BcBSK18, and BcBSK20 showing values above 80.

Table 1. Characteristics and physicochemical properties of BcBSK gene family members.

Transcript_ ID	Gene ID	Protein length (aa)	Molecular weight (kDa)	Theoretical isoelectric point	Instability Index	Aliphatic Index	Grand average of hydropathicity	Subcellular localization
BraC01g028750	*BcBSK 1*	465	52.287	6.25	49.54	78.32	-0.389	Cell membrane
BraC10g000250	*BcBSK 2*	486	55.019	5.97	42.01	82.94	-0.325	Cell membrane
BraC09g014070	*BcBSK 3*	485	54.199	6.05	46.21	76.12	-0.429	Cell membrane
BraC10g016170	*BcBSK 4*	491	55.008	5.71	37.45	78.9	-0.35	Cell membrane
BraC08g016140	*BcBSK 5*	505	56.470	5.58	42.02	74.63	-0.471	Cell membrane
BraC09g010080	*BcBSK 6*	466	52.702	6.51	36.65	77.68	-0.405	Cell membrane
BraC10g035500	*BcBSK 7*	491	55.838	5.46	46.72	77.52	-0.401	Cell membrane
BraC09g012510	*BcBSK 8*	488	54.734	5.96	47.37	78.83	-0.411	Cell membrane
BraC03g034580	*BcBSK 9*	506	57.918	8.74	41.99	79.25	-0.325	Cell membrane
BraC01g009520	*BcBSK 10*	496	55.837	5.35	39.34	81.59	-0.370	Cell membrane
BraC04g006170	*BcBSK 11*	490	55.099	6.26	36.49	78.08	-0.392	Cell membrane

 doi:10.20944/preprints202604.0627.v1

BraC05g043990	*BcBSK12*	491	55.546	5.48	46.43	80.26	-0.354	Cell membrane
BraC03g044980	*BcBSK13*	465	52.416	5.17	42.61	78.67	-0.334	Cell membrane
BraC01g003110	*BcBSK14*	511	57.058	5.66	40.16	67.42	-0.543	Cell membrane
BraC01g045810	*BcBSK15*	490	55.514	6.23	50.92	79.08	-0.335	Cell membrane
BraC07g032910	*BcBSK16*	481	54.548	5.86	34.87	78.88	-0.435	Cell membrane
BraC06g048940	*BcBSK17*	489	54.908	5.62	39.56	82.23	-0.400	Cell membrane
BraC09g001240	*BcBSK18*	484	54.652	5.58	42.43	80.02	-0.411	Cell membrane
BraC03g030580	*BcBSK19*	491	55.186	5.77	42.40	79.06	-0.418	Cell membrane
BraC02g011510	*BcBSK20*	489	54.672	5.52	37.61	80.25	-0.316	Cell membrane

[1] Protein length, Molecular weight (MW), Theoretical isoelectric point (pI), Instability Index, Aliphatic Index, and Grand average of hydropathicity (GRAVY) were calculated using the ExPASy ProtParam tool. Subcellular localization was predicted using DeepLoc 2.1.

3.2. Phylogenetic Analysis of the BcBSK Gene Family

An unrooted phylogenetic tree was constructed based on 20 BSK protein sequences from NHCC and 120 homologous sequences derived from 15 representative species (Figure 1). These species encompassed bryophytes, ferns, gymnosperms, dicotyledons, and monocotyledons.

Phylogenetic analysis grouped the 140 BSK proteins into five subgroups (I–V), with strong support at the major nodes. Distinct differences in species composition were observed among subgroups. Subgroup IV consisted exclusively of monocot species, whereas subgroup V contained only dicot species. In NHCC, the 20 BcBSK proteins were distributed across four subgroups: subgroup I included BcBSK5, BcBSK6, BcBSK13, BcBSK14, and BcBSK16; subgroup II included BcBSK10 and BcBSK17; subgroup III comprised BcBSK4, BcBSK7, BcBSK9, BcBSK11, BcBSK12, BcBSK15, and BcBSK20; and subgroup V contained BcBSK1, BcBSK2, BcBSK3, BcBSK8, BcBSK18, and BcBSK19. Notably, BSK members from the bryophyte *Physcomitrium patens* were predominantly clustered within subgroup II.

 doi:10.20944/preprints202604.0627.v1

The number of *BSK* genes varied among species. Except for *Thuja plicata*, which contained only three members, all other species possessed at least five *BSK* genes. Specifically, NHCC, *Nicotiana tabacum*, *Populus trichocarpa*, and *Arabidopsis thaliana* contained 20, 18, 14, and 12 members, respectively.

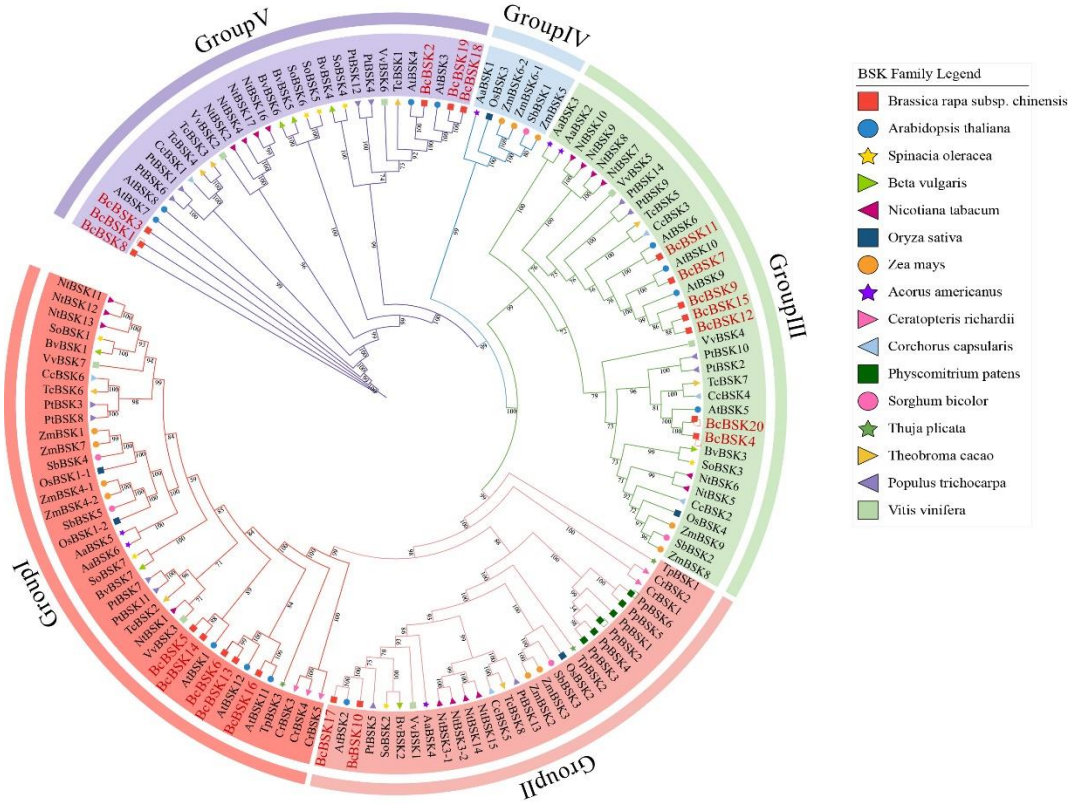

Figure 1. Phylogenetic analysis of the BSK gene family. An unrooted maximum likelihood (ML) phylogenetic tree was constructed using 20 BSK proteins from NHCC and 120 homologs from 15 representative plant species. The proteins were grouped into five clades (I–V), indicated by branch colors. Species are distinguished by colors and symbols as shown in the legend. BcBSK proteins are highlighted in red. Bootstrap support values are shown at the nodes.

3.3. Chromosomal Localization, Synteny, and Ka/Ks Analysis of the BcBSK Gene Family

The chromosomal distribution and syntenic relationships of *BcBSK* genes are presented in Figure 2 and 3, respectively. The 20 *BcBSK* genes were unevenly distributed across 10 chromosomes in NHCC. Chromosomes A09 and A01 each harbored four genes: A09 (*BcBSK3*, *BcBSK6*, *BcBSK8*, and *BcBSK18*) and A01 (*BcBSK1*, *BcBSK10*, *BcBSK14*, and *BcBSK15*). Chromosomes A03 and A10 each contained three genes: A03 (*BcBSK9*, *BcBSK13*, and *BcBSK19*) and A10 (*BcBSK2*, *BcBSK4*, and *BcBSK7*). The remaining six genes were distributed across six different chromosomes.

Intraspecies synteny analysis identified 16 collinear gene pairs (Figure 3), forming multiple interchromosomal relationships and a relatively complex interaction pattern. Ka/Ks analysis showed that all collinear gene pairs had Ka/Ks ratios < 1 (Table 2), indicating that they have undergone purifying selection during evolution.

 doi:10.20944/preprints202604.0627.v1

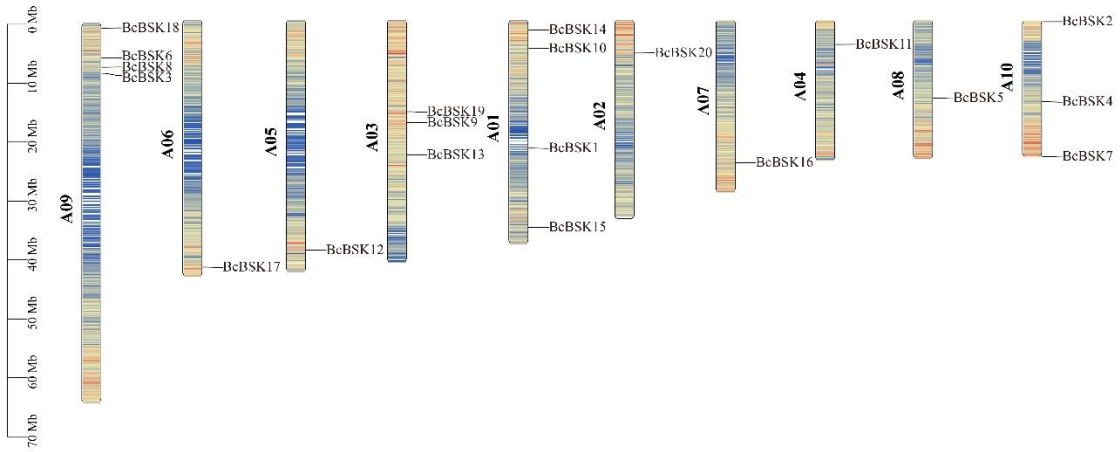

Figure 2. Chromosomal distribution of the BcBSK gene family. The physical positions of 20 *BcBSK* genes on NHCC chromosomes are shown. Chromosomes are represented as vertical bars and labeled A01–A10, with genomic coordinates indicated in megabases (Mb). Gene names are displayed at their respective chromosomal locations.

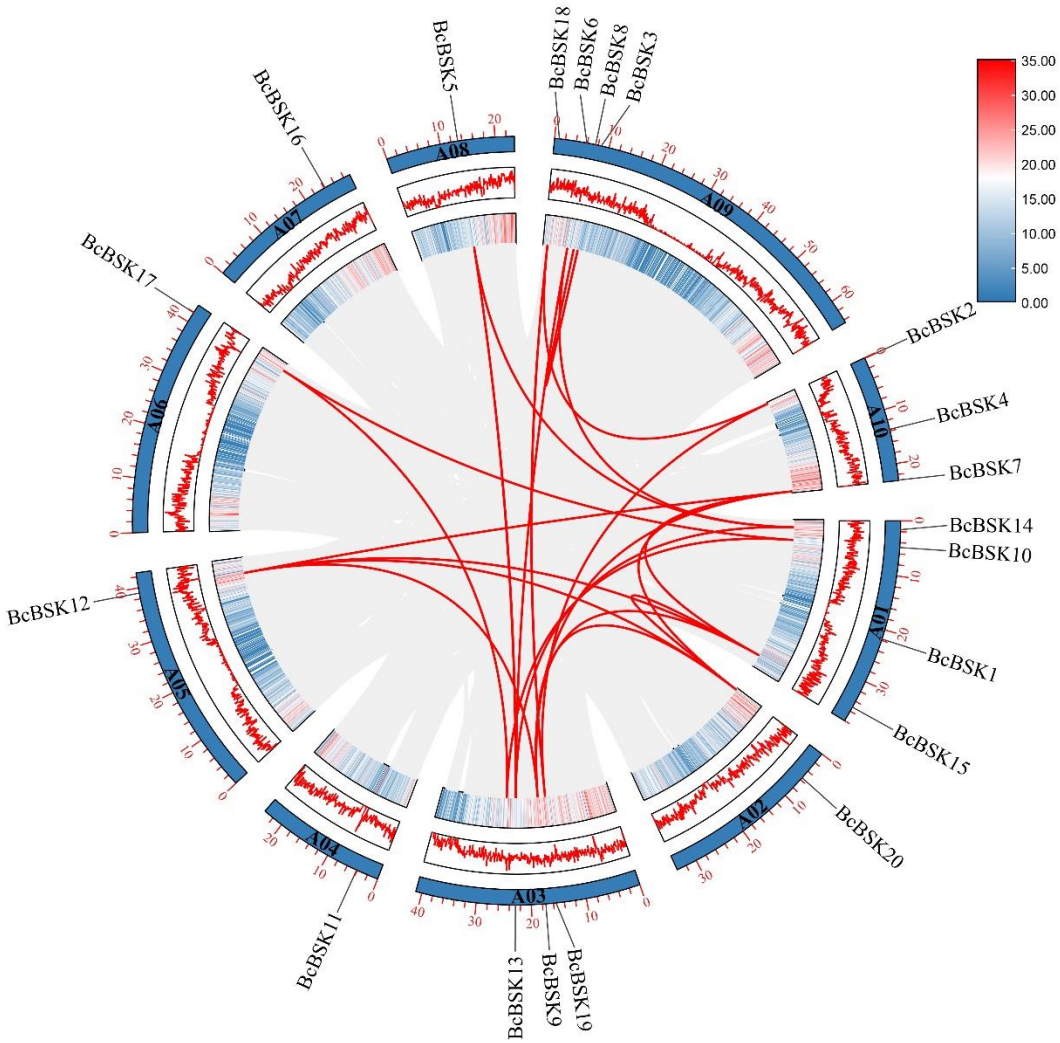

Figure 3. Intraspecies synteny analysis of the BcBSK gene family. From the outer to inner layers, the circles represent chromosome distribution, gene density, and syntenic relationships, respectively. Red lines indicate collinear gene pairs among *BcBSK* members, reflecting gene duplication and expansion within the genome.

 doi:10.20944/preprints202604.0627.v1

Table 2. Ka/Ks analysis of collinear gene pairs in the BcBSK gene family.

gene1	gene2	Ka	Ks	Ka/Ks	purifying selection
BcBSK15	*BcBSK9*	0.07089	0.274025	0.258699	YES
BcBSK14	*BcBSK13*	0.244432	0.332851	0.734357	YES
BcBSK15	*BcBSK12*	0.073853	0.325205	0.227096	YES
BcBSK10	*BcBSK17*	0.064546	0.591024	0.109211	YES
BcBSK14	*BcBSK5*	0.057806	0.206685	0.279683	YES
BcBSK14	*BcBSK6*	0.239543	0.319251	0.750328	YES
BcBSK15	*BcBSK7*	0.118482	0.572055	0.207116	YES
BcBSK9	*BcBSK12*	0.088034	0.320583	0.274605	YES
BcBSK13	*BcBSK5*	0.194841	0.476209	0.40915	YES
BcBSK19	*BcBSK18*	0.023446	0.282712	0.082934	YES
BcBSK13	*BcBSK6*	0.118487	0.239274	0.495192	YES
BcBSK9	*BcBSK7*	0.157136	0.415494	0.378191	YES
BcBSK19	*BcBSK2*	0.172094	0.422767	0.407066	YES
BcBSK12	*BcBSK7*	0.129434	0.636526	0.203345	YES
BcBSK8	*BcBSK3*	0.016925	0.243114	0.069616	YES
BcBSK18	*BcBSK2*	0.131279	0.603695	0.217459	YES

[1] Ka and Ks represent nonsynonymous and synonymous substitution rates, respectively. The Ka/Ks ratio was used to assess selection pressure: Ka/Ks < 1 indicates purifying selection, Ka/Ks = 1 indicates neutral evolution, and Ka/Ks > 1 indicates positive selection. "Purifying selection" denotes gene pairs subjected to purifying selection.

3.4. Gene Structure and Conserved Domain Analysis of the BcBSK Gene Family

The structural features of the BcBSK gene family were analyzed (Figure 4). Conserved motif analysis (Figure 4B) showed that most proteins contained eight conserved motifs (Motifs 1–8), with a generally consistent distribution pattern. However, some members, including *BcBSK6*, *BcBSK13*, and *BcBSK16*, contained only seven motifs, and *BcBSK6* and *BcBSK13* exhibited highly similar motif compositions.

Gene structure analysis (Figure 4C) indicated that most *BcBSK* genes contained nine exons. Specifically, *BcBSK3*, *BcBSK4*, *BcBSK8*, *BcBSK9*, *BcBSK15*, and *BcBSK20* each contained ten exons, whereas *BcBSK1*, *BcBSK17*, and *BcBSK16* contained eleven, eight, and seven exons, respectively. Similar exon–intron organization patterns were observed in several gene pairs, such as *BcBSK6*/*BcBSK13*, *BcBSK4*/*BcBSK20*, *BcBSK12*/*BcBSK15*, and *BcBSK18*/*BcBSK19*.

Domain analysis (Figure 4D) showed that all BcBSK proteins possessed a conserved kinase domain at the N-terminus and tetratricopeptide repeat (TPR) domains at the C-terminus, indicating a highly conserved domain architecture across the family.

 doi:10.20944/preprints202604.0627.v1

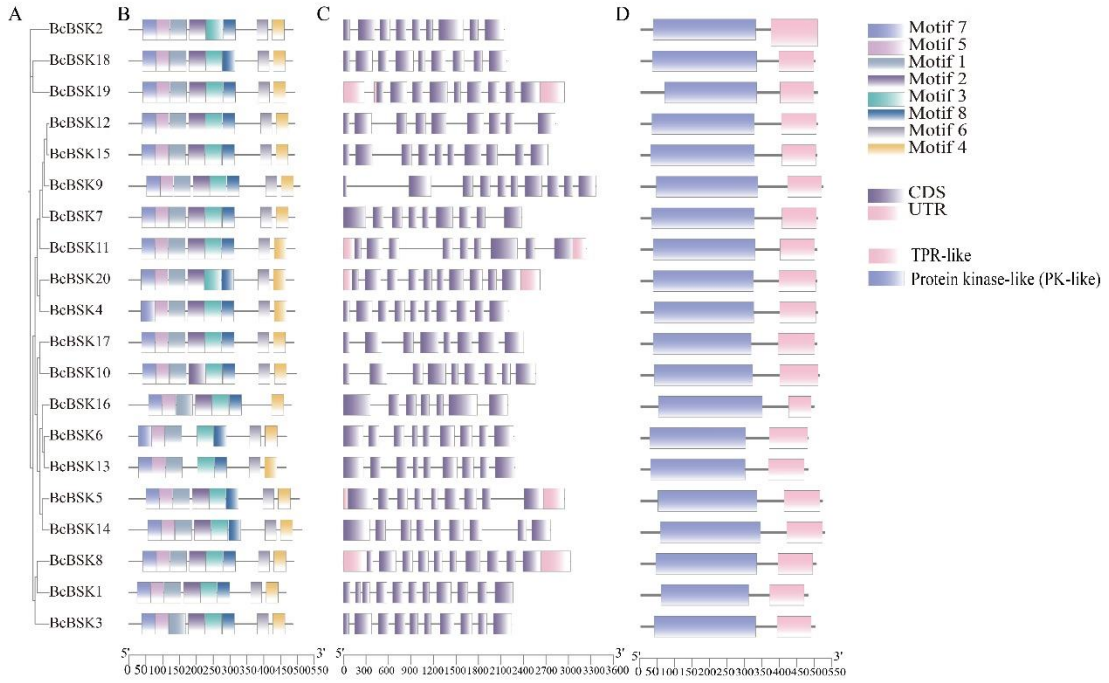

Figure 4. Conserved motifs, gene structure, and domain organization of the BcBSK gene family. (A) Phylogenetic relationships; (B) conserved motif composition; (C) exon–intron structures; (D) protein domain organization. Different colors represent distinct motifs or domain types.

3.5. Cis-acting Element Analysis of BcBSK Gene Promoters

The 2000 bp upstream promoter regions of *BcBSK* genes were analyzed using the PlantCARE database, and the results are shown in Figure 5. All promoters contained core cis-elements, including the TATA-box and CAAT-box. In addition, multiple cis-acting elements associated with light responsiveness, abiotic stress, hormone responses, and growth and development were identified.

Among these, light-responsive elements were the most abundant, followed by hormone-responsive elements. Notably, ABRE, as well as CGTCA-motif and TGACG-motif, were widely distributed across multiple promoters. Elements related to auxin, salicylic acid, and gibberellin responses were also detected.

Stress-related elements were also prevalent. ARE elements were identified in multiple genes, with *BcBSK5* containing the highest number (10). The G-box element was enriched in certain genes, with eight and seven copies identified in *BcBSK13* and *BcBSK1*, respectively. Additionally, elements associated with low-temperature responsiveness (LTR), drought inducibility (MBS), and defense and stress responsiveness (TC-rich repeats) were detected.

Furthermore, several elements related to growth and development were identified, including those involved in meristem regulation, endosperm expression, and cell cycle control.

 doi:10.20944/preprints202604.0627.v1

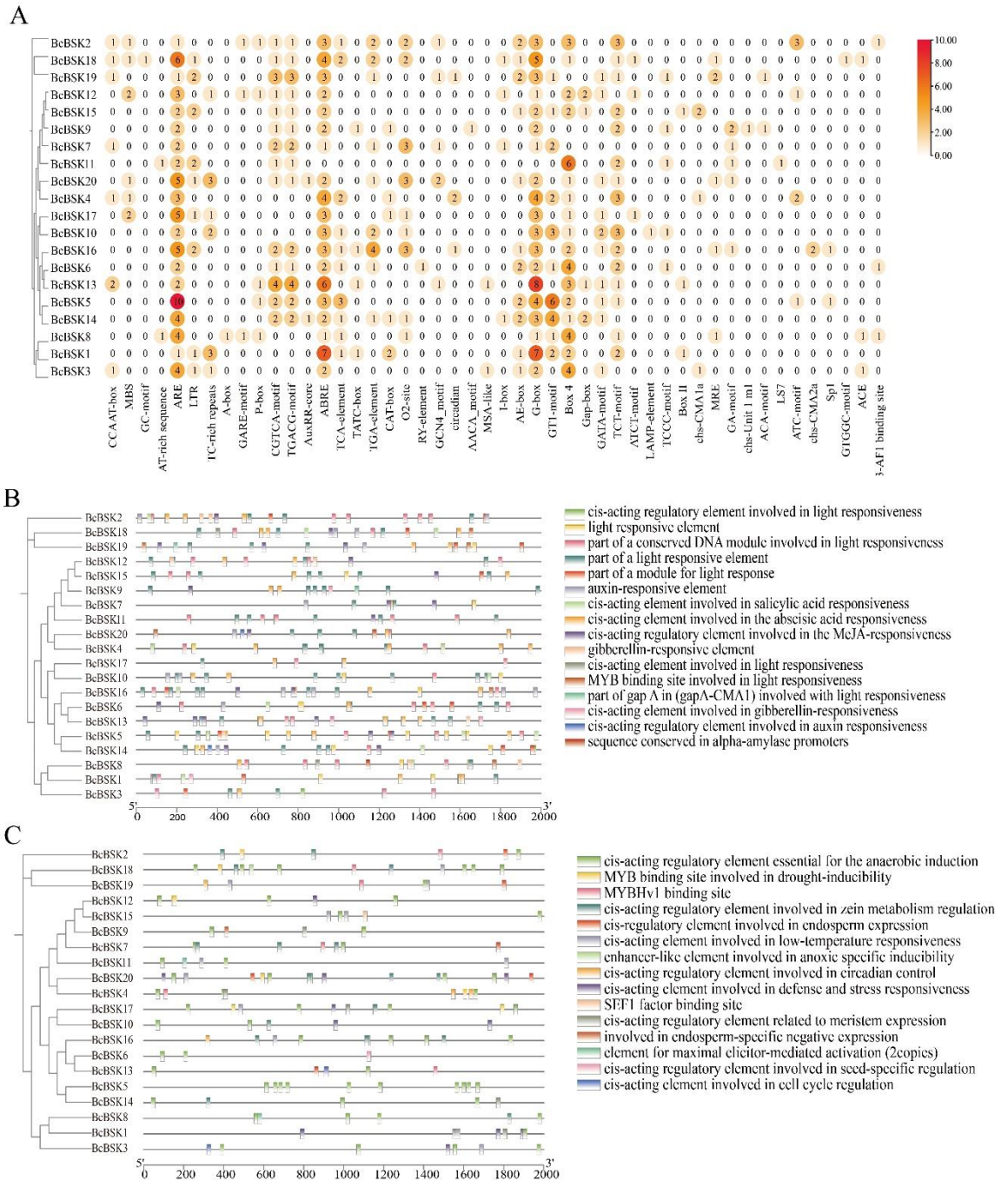

Figure 5. Cis-acting element analysis of *BcBSK* gene promoters. (A) Types and numbers of cis-acting elements; (B–C) distribution of functional elements within promoter regions. Different colors represent different categories of regulatory elements.

3.6. Protein-Protein Interaction Network Analysis of BcBSK Proteins

The protein–protein interaction (PPI) network of BcBSK proteins is shown in Figure 6. The 20 members exhibited a radial distribution pattern. BcBSK2, BcBSK5, BcBSK14, and BcBSK18 were located in the central region, with darker node colors, whereas the remaining proteins were distributed across two outer layers. From the periphery to the center, node color intensity increased, corresponding to higher interaction density and connectivity.

Further analysis indicated that BcBSK proteins interacted extensively with multiple members of the BRAP family, forming relatively concentrated interaction clusters within the network.

 doi:10.20944/preprints202604.0627.v1

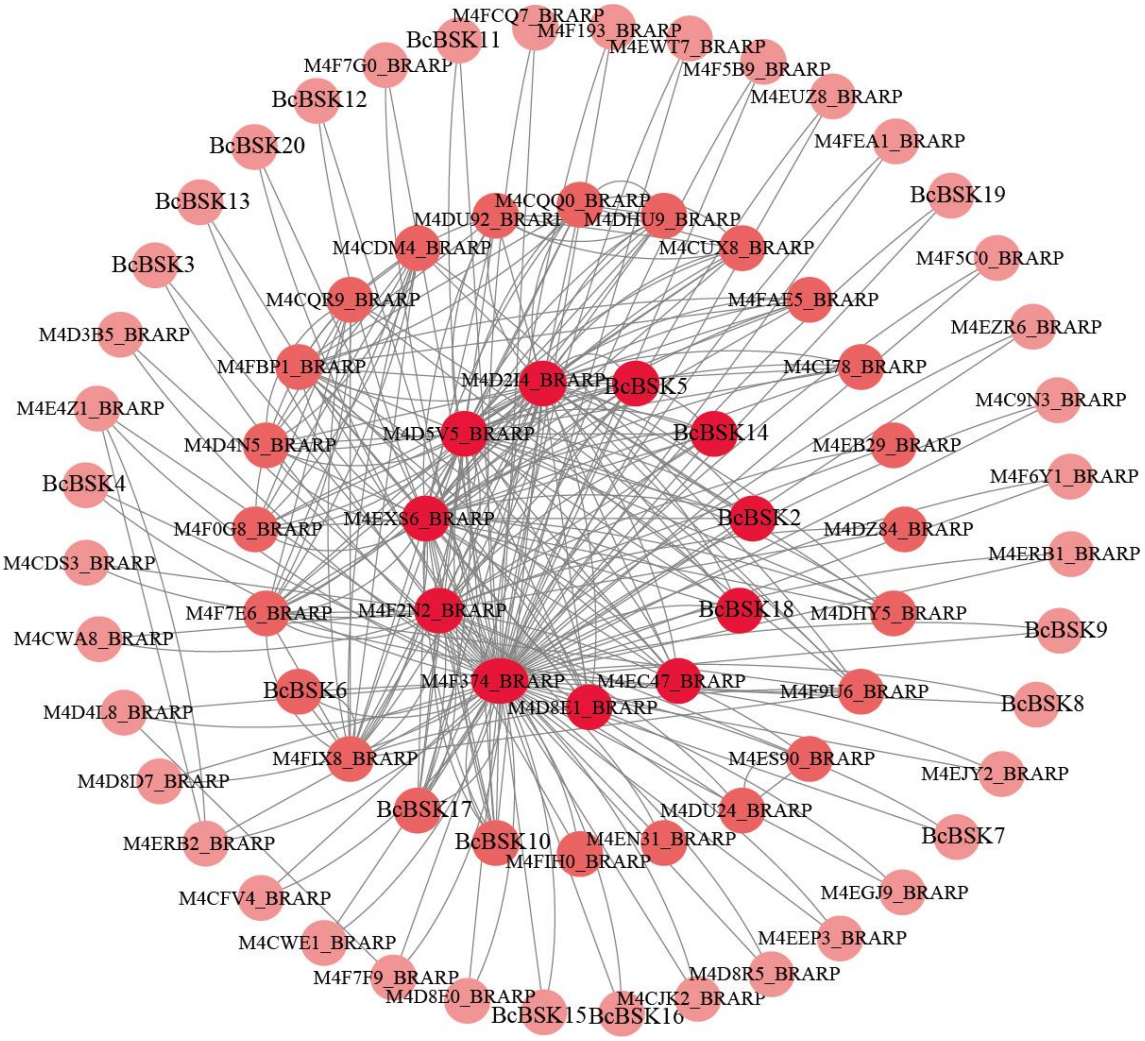

Figure 6. Protein–protein interaction network of BcBSK proteins. The network was constructed based on homology-based mapping. Nodes represent proteins, and edges indicate potential interactions. Node color reflects network connectivity, with darker colors indicating higher interaction density.

3.7. Expression Profile Analysis of the BcBSK Gene Family Under Heat Stress

Heatmap analysis showed that *BcBSK* genes exhibited clear cultivar-specific differences and dynamic temporal expression patterns under heat stress (Figure 7). In the heat-sensitive cultivar "Aijiaohuang", gene expression displayed greater variability, with pronounced changes over time.

BcBSK1 was consistently upregulated at 6 h ($log_2FC = 1.71$) and 24 h ($log_2FC = 2.56$), with higher expression at 24 h. Similarly, *BcBSK2* was upregulated at both time points ($log_2FC = 1.76$ and 2.25). *BcBSK18* showed marked upregulation at 6 h ($log_2FC = 1.80$) and remained upregulated at 24 h despite a slight decrease ($log_2FC = 1.01$). In contrast, *BcBSK9* and *BcBSK20* were downregulated at both time points, with log_2FC values of −4.32 and −1.59 for *BcBSK9*, and −2.57 and −2.91 for *BcBSK20* at 6 h and 24 h, respectively.

In the heat-tolerant cultivar "SHI", most genes exhibited relatively stable expression patterns. *BcBSK2* was upregulated at 6 h ($log_2FC = 1.12$) and 24 h ($log_2FC = 1.73$), although the magnitude was lower than in "Aijiaohuang". *BcBSK15* was downregulated at 6 h ($log_2FC = -2.19$) but showed slight upregulation at 24 h ($log_2FC = 0.17$), indicating a reversal in expression trend. The remaining genes showed no pronounced changes.

 doi:10.20944/preprints202604.0627.v1

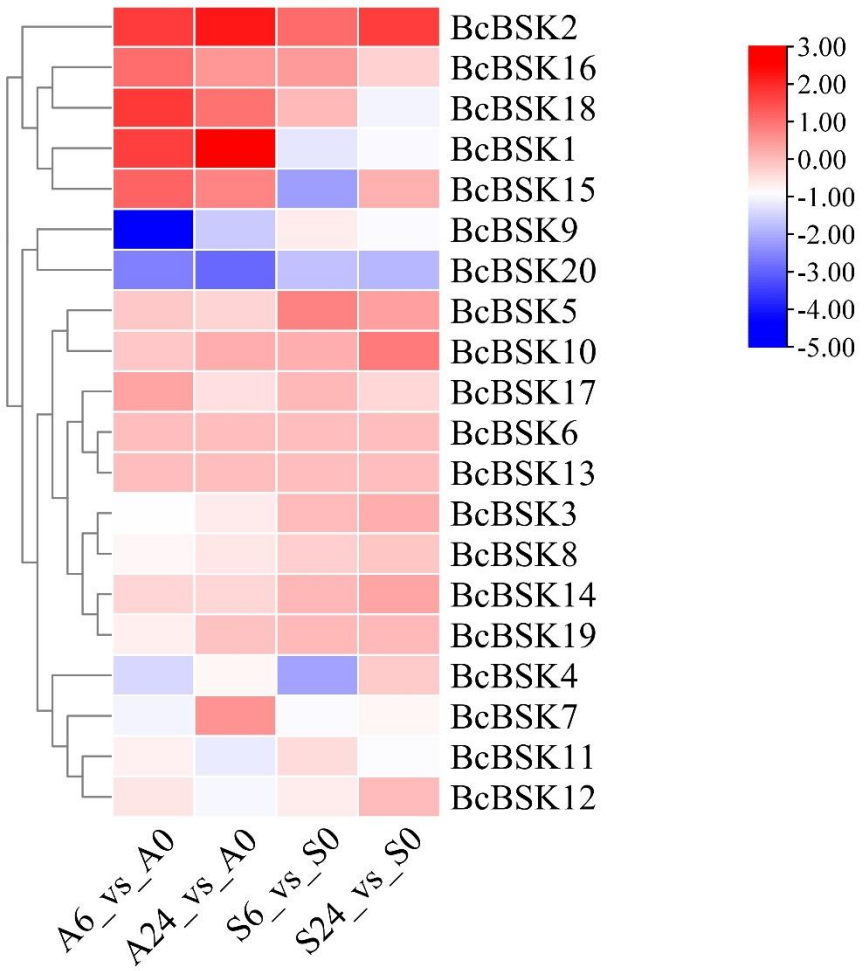

Figure 7. Expression profile of the BcBSK gene family. Colors represent relative expression levels, with red indicating upregulation ($log_2FC > 0$) and blue indicating downregulation ($log_2FC < 0$). The dendrogram on the left represents hierarchical clustering of genes.

3.8. qRT–PCR Validation of Expression Changes in BcBSK Genes

To validate the transcriptomic data, selected *BcBSK* genes were analyzed by qRT–PCR under heat stress at 0, 6, and 24 h (Figure 8).

In the heat-sensitive cultivar "Aijiaohuang", the expression trends of the selected genes were consistent with the transcriptomic results. In the heat-tolerant cultivar "SHI", gene expression showed only minor fluctuations during the 0-24 h period, consistent with the relatively stable expression patterns observed in the transcriptome analysis.

 doi:10.20944/preprints202604.0627.v1

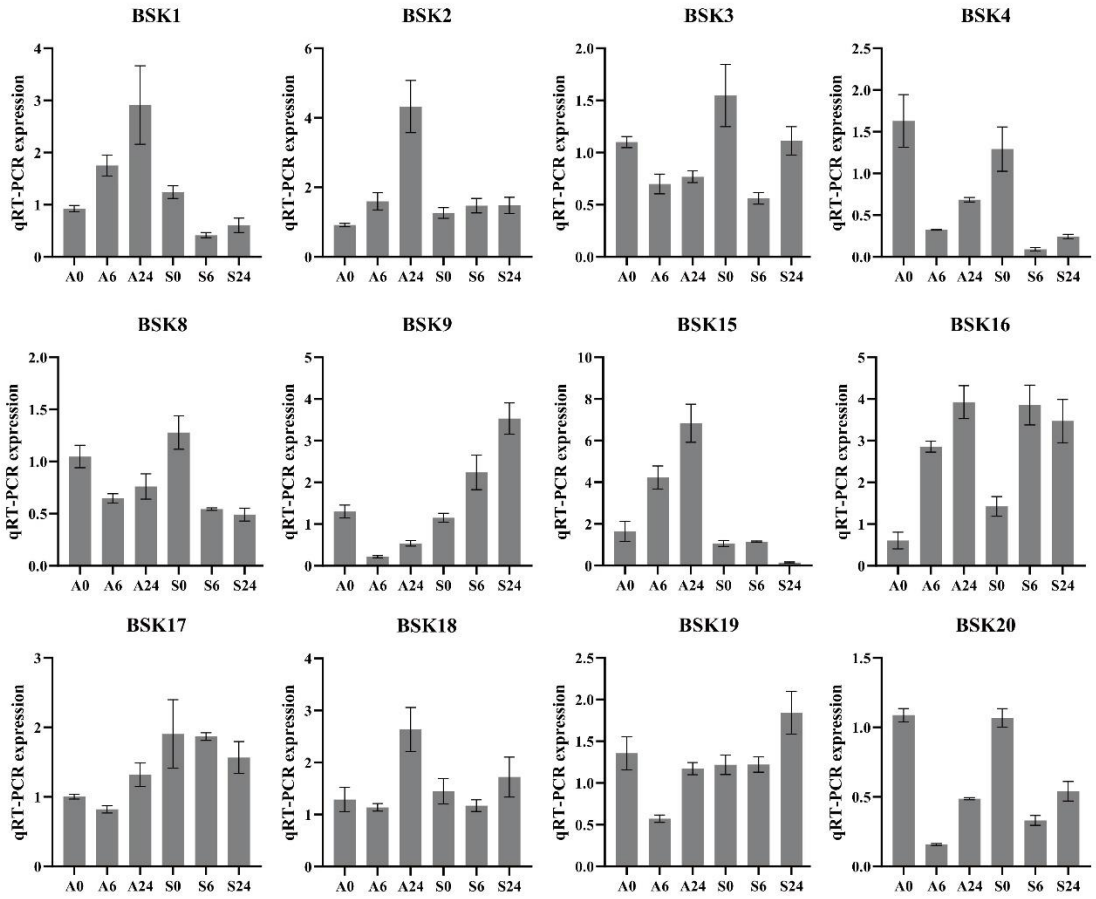

Figure 8. qRT–PCR validation of *BcBSK* gene expression under heat stress. Relative expression levels at different time points (0, 6, and 24 h) are presented as bar charts, with error bars indicating the standard error (SE). Expression levels were calculated using the $2^{-\Delta\Delta Ct}$ method. A and S denote the heat-sensitive cultivar "Aijiaohuang" and the heat-tolerant cultivar "SHI", respectively.

3.9. Physiological Responses of NHCC Under Heat Stress

The effects of exogenous BR treatment on physiological parameters in leaves of the heat-sensitive cultivar "Aijiaohuang" under heat stress are shown in Figure 9. Antioxidant enzyme activities exhibited clear time-dependent responses to different BR concentrations.

For catalase (CAT), the 0.1 mg·L^{-1} treatment maintained relatively high activity throughout the 0-9 d period; the 0.5 mg·L^{-1} treatment showed pronounced increases at 3 d and 6 d; whereas the 1.0 mg·L^{-1} treatment showed significant differences only at 9 d ($P < 0.05$). Peroxidase (POD) activity was higher in all BR-treated groups than in the control at 0 d ($P < 0.05$). The 0.5 mg·L^{-1} treatment maintained the highest POD activity from 3 to 9 d. Superoxide dismutase (SOD) activity showed a similar trend, with the 0.5 mg·L^{-1} treatment exhibiting the highest values at all time points and peaking at 6 d.

Regarding membrane lipid peroxidation and osmotic regulation, both the 0.1 mg·L^{-1} and 0.5 mg·L^{-1} treatments reduced malondialdehyde (MDA) content at all time points, with the greatest reduction observed at 6 d under the 0.5 mg·L^{-1} treatment ($P < 0.05$). In contrast, the 1.0 mg·L^{-1} treatment showed relatively minor changes. Proline content remained consistently higher under the 0.5 mg·L^{-1} treatment.

Photosynthetic pigment contents are presented in Table 3. The 0.5 mg·L^{-1} treatment increased chlorophyll a, chlorophyll b, carotenoid, and total chlorophyll contents at most time points ($P < 0.05$). The 1.0 mg·L^{-1} treatment showed increases at 6 d and 9 d, whereas the 0.1 mg·L^{-1} treatment showed

 doi:10.20944/preprints202604.0627.v1

minimal changes. The chlorophyll a/b ratio was lowest under the 0.5 mg·L^{-1} treatment at 0 d and 3 d, with no significant differences observed at later stages.

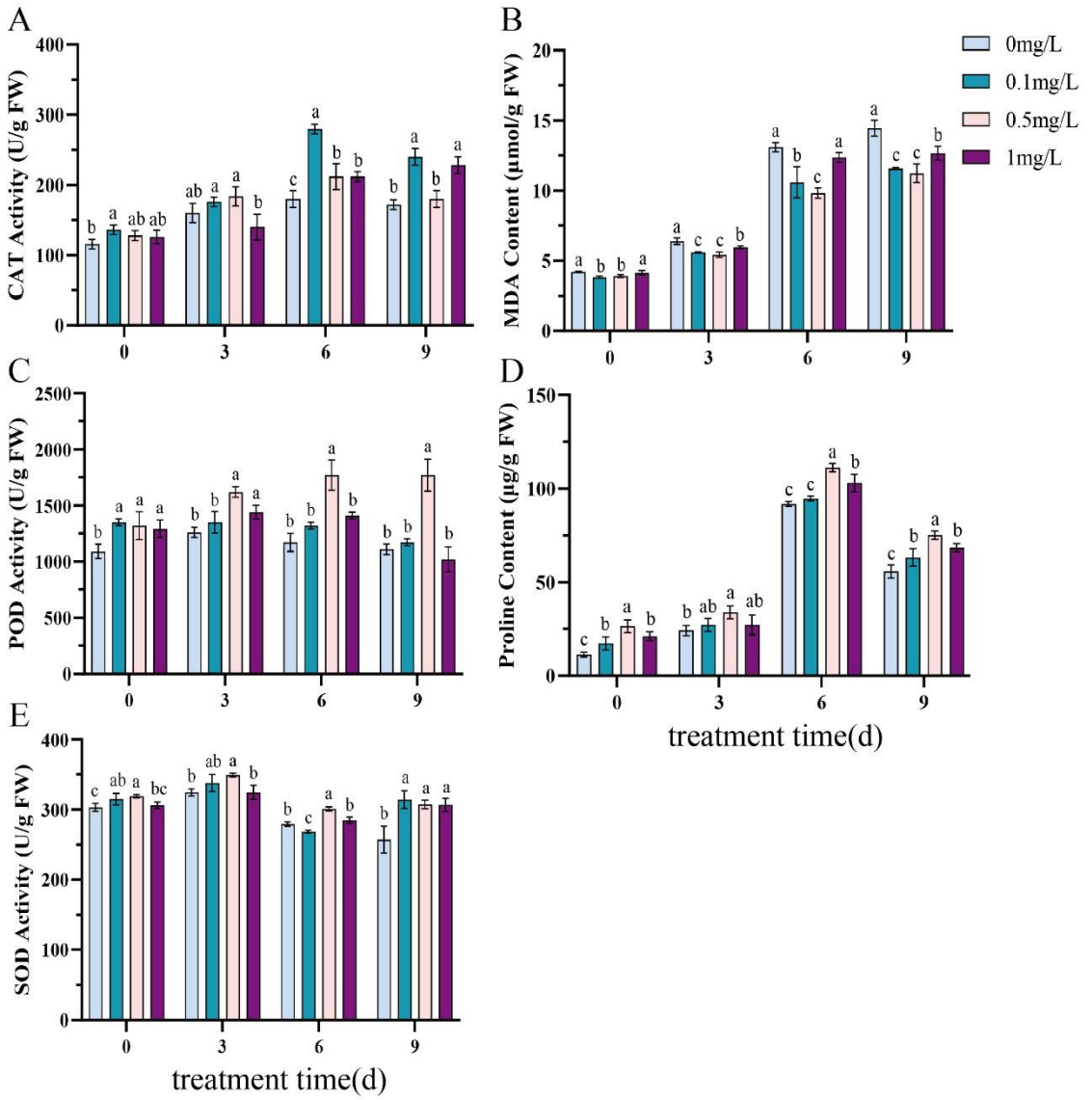

Figure 9. Effects of exogenous BR treatment on physiological parameters in leaves of the heat-sensitive cultivar "Aijiaohuang" under heat stress. (A) CAT activity; (B) MDA content; (C) POD activity; (D) proline content; (E) SOD activity. BR concentrations were 0, 0.1, 0.5, and 1.0 mg·L^{-1}. Different letters indicate significant differences among treatments at the same time point ($P < 0.05$). Error bars represent the standard error (SE).

Table 3. Effects of exogenous BR on photosynthetic pigment contents in leaves of the heat-sensitive cultivar "Aijiaohuang" under heat stress.

Time (d)	BR (mg/L)	Chlorophyll a (mg/g)	Chlorophyll b (mg/g)	Carotenoid (mg/g)	Total Chlorophyll (mg/g)	Chlorophyll a/b
0	0.00	0.503±0.015c	0.191±0.004c	0.012±0.001c	0.694±0.017c	2.633±0.083a
	0.10	0.522±0.017bc	0.215±0.026bc	0.015±0.001b	0.737±0.010c	2.461±0.352a
	0.50	0.560±0.017a	0.360±0.010a	0.018±0.000a	0.920±0.027a	1.560±0.008b

 doi:10.20944/preprints202604.0627.v1

3	1.00	0.539±0.001ab	0.248±0.034b	0.016±0.000ab	0.786±0.034b	2.202±0.308a
	0.00	0.416±0.012c	0.124±0.005c	0.010±0.002d	0.540±0.021d	3.362±0.116a
	0.10	0.516±0.008a	0.198±0.014b	0.021±0.000c	0.714±0.013b	2.621±0.189b
	0.50	0.511±0.003a	0.292±0.016a	0.083±0.002a	0.803±0.016a	1.756±0.095c
	1.00	0.478±0.009b	0.187±0.011b	0.056±0.008b	0.664±0.003c	2.571±0.206b
6	0.00	0.458±0.016b	0.155±0.060c	0.031±0.005b	0.613±0.021bc	2.952±0.073a
	0.10	0.394±0.045c	0.196±0.013b	0.020±0.000c	0.590±0.036c	2.027±0.355b
	0.50	0.527±0.012a	0.261±0.022a	0.078±0.000a	0.788±0.034a	2.028±0.123b
	1.00	0.479±0.009ab	0.181±0.017bc	0.083±0.009a	0.660±0.011b	2.667±0.277a
9	0.00	0.379±0.012ab	0.211±0.016b	0.005±0.001d	0.591±0.017b	1.804±0.165a
	0.10	0.364±0.010b	0.200±0.012b	0.011±0.001c	0.563±0.008c	1.823±0.148a
	0.50	0.393±0.002a	0.237±0.008a	0.068±0.003a	0.631±0.010a	1.659±0.050a
	1.00	0.390±0.007a	0.237±0.008a	0.053±0.003b	0.627±0.002a	1.647±0.084a

[1] Data are presented as mean ± Standard Error (SE). Different lowercase letters indicate significant differences at $P < 0.05$ within the same treatment or time point. Chlorophyll a, chlorophyll b, carotenoid, and total chlorophyll represent the contents of chlorophyll a, chlorophyll b, carotenoids, and total chlorophyll, respectively.

4. Discussion

4.1. Evolution, Structure, and Functional Divergence of the BcBSK Gene Family in NHCC

BSK genes, as early components of the BR signaling pathway, play essential regulatory roles in plant growth, development, and stress responses. In the present study, 20 *BcBSK* genes were identified in NHCC. Phylogenetic analysis indicates that this gene family exhibits lineage-specific diversification during evolution. Specifically, subgroup IV comprises exclusively monocotyledonous species, whereas subgroup V consists entirely of dicotyledonous species; the remaining subgroups include members from both lineages. This distribution pattern is consistent with previous reports [3,15], suggesting that the BSK gene family has undergone evolutionary divergence across plant lineages. The presence of lineage-specific subgroups implies independent gene retention in different evolutionary branches, whereas the mixed composition of other subgroups reflects a relatively high level of conservation among certain members. Whole-genome duplication is widely recognized as a major driver of gene family expansion in plants [38–40], and duplicated genes may undergo differential retention and functional divergence, ultimately shaping the observed family structure.

Within this evolutionary framework, the expansion of the BcBSK gene family in NHCC appears to be primarily associated with whole-genome duplication or large-scale segmental duplication events. Synteny analysis reveals complex collinearity relationships among family members, and the consistently low Ka/Ks ratios (<1) indicate that these genes are under strong purifying selection. Subcellular localization prediction shows that all BcBSK proteins are localized to the plasma membrane. This uniform localization not only reflects structural conservation but also supports their

 doi:10.20944/preprints202604.0627.v1

functional roles in BR signaling, where membrane association is essential for interactions with receptors such as BRI1 and other signaling components.

From a structural perspective, all BcBSK proteins contain conserved kinase domains and tetratricopeptide repeat (TPR) domains, indicating that their core functional modules remain highly conserved. This structural feature, commonly observed in BSK proteins, highlights its fundamental importance in signal transduction. Protein–protein interaction network analysis further shows that these proteins are mainly associated with cytoplasmic components of the BR signaling pathway, suggesting a high degree of functional convergence. Notably, BcBSK2, BcBSK5, BcBSK14, and BcBSK18 are located at central positions in the interaction network, implying that they may play key regulatory roles.

Based on previously reported functions of different subgroups, the potential roles of BcBSK members can be inferred. Subgroup V shows high sequence similarity to key BR signaling components in *Arabidopsis thaliana* (e.g., AtBSK3, AtBSK4, AtBSK7, and AtBSK8) and is therefore likely involved primarily in BR signal transduction [3]. In contrast, subgroup I homologs have been implicated in immune responses [24–26], drought and salt stress responses [41], and abscisic acid (ABA) signaling [23], suggesting broader roles in stress adaptation. Subgroup III appears more functionally diverse, with homologs associated with heat stress [15], root development [13], seed development [17], and salt stress responses [42], indicating a role in coordinating growth and environmental responses. Subgroup II, by comparison, is more closely associated with fundamental growth regulation; for example, OsBSK2 regulates grain size in rice, suggesting relatively conserved functions within this subgroup [25].

Promoter analysis further reveals regulatory divergence among *BcBSK* genes. For example, the promoter region of *BcBSK5* is enriched in anaerobic-responsive elements, whereas *BcBSK13* and *BcBSK1* contain a higher abundance of light-responsive elements. Such variation in cis-element composition may contribute to transcriptional diversity, enabling different family members to respond to distinct environmental and endogenous signals, thereby facilitating functional differentiation and coordination within the gene family.

4.2. Alleviating Effects of Exogenous BRs on Heat Stress in NHCC

Under heat stress conditions, exogenous application of BRs partially alleviates physiological damage in the heat-sensitive cultivar “Aijiaohuang”. In the present study, comparison among different concentrations indicates that 0.5 mg·L^{-1} BR provides a relatively stable protective effect throughout the stress period, particularly during the critical stage from 3 to 6 d.

From a physiological perspective, this protective effect is closely associated with sustained activation of the antioxidant system. The activities of key enzymes, including superoxide dismutase (SOD), peroxidase (POD), and catalase (CAT), remain at relatively high levels following BR treatment, suggesting enhanced reactive oxygen species (ROS) scavenging capacity and reduced oxidative damage [43,44]. Meanwhile, the continuous accumulation of proline and the decrease in malondialdehyde (MDA) content indicate improved osmotic adjustment and reduced membrane lipid peroxidation [45], which contribute to maintaining cellular integrity.

With respect to photosynthetic performance, BR treatment also affects the contents of chlorophyll a, chlorophyll b, and carotenoids. These pigments are generally maintained at higher levels under stress conditions, indicating a protective role in preserving the photosynthetic apparatus [46,47]. These physiological processes are unlikely to operate independently; instead, they appear to act in a coordinated manner to enhance plant adaptation to elevated temperatures. Notably, the regulatory effects of BR exhibit clear concentration dependence. Among the tested treatments, 0.5 mg·L^{-1} appears to be more effective, possibly because it better matches the endogenous BR signaling range in NHCC, thereby promoting downstream stress-response pathways. However, this interpretation still requires further validation at the molecular level.

 doi:10.20944/preprints202604.0627.v1

4.3. Association Between BcBSK Expression Patterns and Physiological Responses to Exogenous BR

Integrated analysis of gene expression profiles and physiological parameters provides important insights into the role of BR in heat stress responses. In the heat-sensitive cultivar "Aijiaohuang", genes such as *BcBSK1*, *BcBSK2*, and *BcBSK18* show rapid upregulation during the early stage of stress (6–24 h), whereas BR-induced physiological changes are mainly observed during the intermediate stage (3–6 d). This temporal pattern suggests that certain *BcBSK* members are activated at early stages of stress and may contribute to the establishment of subsequent physiological responses, which is consistent with the role of BSKs as early signaling components in the BR pathway [48].

Further comparison among individual members reveals clear divergence in expression patterns within the BcBSK gene family under heat stress. This variation is partially consistent with their positions in the protein interaction network. Previous studies indicate that BSK proteins participate in BR signal transduction through interactions with multiple downstream components and exhibit functional differentiation across physiological processes [49]. Notably, BcBSK2, BcBSK5, BcBSK14, and BcBSK18, which occupy central positions in the interaction network, show pronounced expression changes under stress conditions, suggesting that they may play key roles in signal transduction. In particular, the sustained upregulation of *BcBSK2* in the heat-sensitive cultivar is consistent with the trends observed in SOD and POD activities under 0.5 mg·L^{-1} BR treatment, indicating a possible link to antioxidant regulation.

Comparison between heat-tolerant and heat-sensitive cultivars further reveals a potential association between *BcBSK* expression patterns and thermotolerance. In the heat-tolerant cultivar "SHI", most genes exhibit relatively stable expression with limited fluctuations during stress, whereas in the heat-sensitive cultivar, several genes display marked expression changes. This contrast may reflect distinct regulatory strategies in response to stress. Similar patterns have been reported in other plant species, where tolerant genotypes tend to maintain more stable and coordinated transcriptional regulation, whereas sensitive genotypes show greater expression variability under stress conditions [50].

In combination with the effects of exogenous BR, it is observed that in the heat-sensitive cultivar, pronounced gene expression changes are accompanied by partial improvement in physiological parameters following BR treatment. This correspondence suggests that BR signaling contributes to the regulation of stress responses in such genotypes. In addition, the presence of multiple hormone-responsive cis-elements in promoter regions indicates that *BcBSK* genes may be co-regulated by different signaling pathways at the transcriptional level. Although this provides a basis for potential hormonal crosstalk, the underlying regulatory mechanisms still require further experimental validation.

Overall, the BcBSK gene family exhibits functional divergence, with different members likely acting at distinct stages and through different mechanisms in response to heat stress. Some genes may primarily participate in early signal perception, whereas others may function in downstream signal transduction and integration. It should be noted that these conclusions are largely based on correlations between expression patterns and physiological data; therefore, further studies with higher temporal resolution and functional validation are required to clarify their precise roles.

5. Conclusions

This study presents a comprehensive genome-wide analysis of the BcBSK gene family in NHCC, clarifying its composition and expansion patterns and providing initial insights into its expression profiles under heat stress. Several *BcBSK* genes show notable responses to BR treatment and heat stress, among which *BcBSK2* exhibits particularly pronounced changes.

By integrating transcriptomic and physiological data, a potential association was observed between early gene expression responses and subsequent physiological changes. In particular, exogenous BR treatment is associated with variations in antioxidant-related parameters, suggesting that the BcBSK gene family may be involved in BR-mediated heat stress responses. However, this

 doi:10.20944/preprints202604.0627.v1

inference is primarily based on correlation analysis, and the underlying regulatory mechanisms remain to be elucidated.

Overall, the BcBSK gene family in NHCC exhibits expression divergence and is likely involved in thermotolerance-related regulatory processes. Further functional validation of key members will be necessary to clarify their roles within the BR signaling network and to support future efforts in improving heat tolerance in this crop.

Supplementary Materials: The following supporting information can be downloaded at the website of this paper posted on Preprints.org., Table S1: Primer sequences used for qRT-PCR; Table S2: List of BSK protein sequences used for phylogenetic analysis.

Author Contributions: Conceptualization, X.L. (Xiaofeng Li) and B.Z.; methodology, L.Y. and J.W.; software, P.Y. and X.L. (Xiang Li); validation, L.Y. and J.W.; formal analysis, L.Y.; investigation, L.Y., J.W., P.Y. and X.L. (Xiang Li); resources, X.L. (Xiaofeng Li) and B.Z.; data curation, L.Y.; writing—original draft preparation, L.Y.; writing—review and editing, X.L. (Xiaofeng Li) and B.Z.; visualization, L.Y.; supervision, X.L. (Xiaofeng Li) and B.Z.; project administration, X.L. (Xiaofeng Li) and B.Z.; funding acquisition, X.L. (Xiaofeng Li) and B.Z. All authors have read and agreed to the published version of the manuscript.

Funding: This research was funded by the Shanghai Science and Technology Development Foundation (grant number 23N11900200) and the Horizontal Scientific Research Project of Anhui Normal University (grant number 2025127).

Data Availability Statement: The RNA-seq data used in this study are publicly available in the NCBI BioProject database under accession number PRJNA1030162. Other data supporting the findings of this study are available from the corresponding author upon reasonable request.

Acknowledgments: The authors thank the Horticultural Research Institute of the Shanghai Academy of Agricultural Sciences for providing plant materials.

Conflicts of Interest: The authors declare no conflicts of interest.

Abbreviations

The following abbreviations are used in this manuscript:

NHCC	Non-heading Chinese cabbage (*Brassica rapa* subsp. *chinensis*)
BR	Brassinosteroid
BSK	BR-signaling kinase
SOD	Superoxide dismutase
POD	Peroxidase
CAT	Catalase
ROS	Reactive oxygen species
MDA	Malondialdehyde
PPI	Protein–protein interaction
HMMs	Hidden Markov models
CDD	Conserved Domain Database
ML	Maximum likelihood
BIC	Bayesian Information Criterion
iTOL	Interactive Tree Of Life
PPI	Protein–protein interaction
FPKM	Fragments Per Kilobase of transcript per Million mapped reads
Ka	nonsynonymous substitution rates
Ks	synonymous substitution rates
qRT–PCR	Quantitative real-time polymerase chain reaction

 doi:10.20944/preprints202604.0627.v1

References

1. Tian, J.; Chang, K.Z.; Lei, Y.X.; Li, S.H.; Wang, J.W.; Huang, C.X.; Zhong, F.L. Genome-Wide Identification of Proline Transporter Gene Family in Non-Heading Chinese Cabbage and Functional Analysis of BchProT1 under Heat Stress. *International Journal of Molecular Sciences* **2024**, *25*, doi:10.3390/ijms25010099.
2. Xin, X.; Li, P.; Zhao, X.; Yu, Y.; Wang, W.; Jin, G.; Wang, J.; Sun, L.; Zhang, D.; Zhang, F.; et al. Temperature-dependent jumonji demethylase modulates flowering time by targeting H3K36me2/3 in Brassica rapa. *Nature Communications* **2024**, *15*, doi:10.1038/s41467-024-49721-z.
3. Li, Z.Y.; Shen, J.Y.; Liang, J.S. Genome-Wide Identification, Expression Profile, and Alternative Splicing Analysis of the Brassinosteroid-Signaling Kinase (BSK) Family Genes in Arabidopsis. *International Journal of Molecular Sciences* **2019**, *20*, doi:10.3390/ijms20051138.
4. Nolan, T.M.; Vukasinovic, N.; Liu, D.R.; Russinova, E.; Yin, Y.H. Brassinosteroids: Multidimensional Regulators of Plant Growth, Development, and Stress Responses. *Plant Cell* **2020**, *32*, 295-318, doi:10.1105/tpc.19.00335.
5. Rao, X.L.; Dixon, R.A. Brassinosteroid Mediated Cell Wall Remodeling in Grasses under Abiotic Stress. *Frontiers in Plant Science* **2017**, *8*, doi:10.3389/fpls.2017.00806.
6. Chakraborty, N.; Ganguly, R.; Sarkar, A.; Dasgupta, D.; Sarkar, J.; Acharya, K.; Burachevskaya, M.; Minkina, T.; Keswani, C. Multifunctional Role of Brassinosteroids in Plant Growth, Development, and Defense. *Journal of Plant Growth Regulation* **2025**, *44*, 2627-2640, doi:10.1007/s00344-024-11593-4.
7. Clouse, S.D. Brassinosteroid Signal Transduction: From Receptor Kinase Activation to Transcriptional Networks Regulating Plant Development. *The Plant Cell* **2011**, *23*, 1219-1230, doi:10.1105/tpc.111.084475.
8. Kim, T.-W.; Guan, S.; Sun, Y.; Deng, Z.; Tang, W.; Shang, J.-X.; Sun, Y.; Burlingame, A.L.; Wang, Z.-Y. Brassinosteroid signal transduction from cell-surface receptor kinases to nuclear transcription factors. *Nature Cell Biology* **2009**, *11*, 1254-1260, doi:10.1038/ncb1970.
9. Li, L.; Mu, T.; Zhang, R.; Zhang, G.; Lyu, J.; Liu, Z.; Luo, S.; Yu, J. The BES1/BZR1 family transcription factor as critical regulator of plant stress resilience. *Plant Stress* **2025**, *15*, 100730, doi:https://doi.org/10.1016/j.stress.2024.100730
10. Liu, F.; Qu, P.-Y.; Li, J.-P.; Yang, L.-N.; Geng, Y.-J.; Lu, J.-Y.; Zhang, Y.; Li, S. Arabidopsis protein S- acyl transferases positively mediate BR signaling through S- acylation of BSK1. *Proceedings of the National Academy of Sciences of the United States of America* **2024**, *121*, doi:10.1073/pnas.2322375121.
11. Yan, J.; Wang, X.; Liu, J.; Wang, Y.; Yue, J.; Wang, W.; Li, Y.; Sun, Y.; Zhang, B.; Tang, W. BSK family kinases are essential for brassinosteroid signaling and suppression of adventitious rooting by repressing the expression of LBD16. *New Phytologist* **2026**, *250*, 283-297, doi:10.1111/nph.70924.
12. Galindo-Trigo, S.; Khandare, V.; Roosjen, M.; Adams, J.; Wangler, A.-M.; Bayer, M.; Borst, J.W.; Smakowska-Luzan, E.; Butenko, M.A. A multifaceted kinase axis regulates plant organ abscission through conserved signaling mechanisms. *Current Biology* **2024**, *34*, doi:10.1016/j.cub.2024.05.057.
13. Ren, H.; Willige, B.C.; Jaillais, Y.; Geng, S.; Park, M.Y.; Gray, W.M.; Chory, J. BRASSINOSTEROID-SIGNALING KINASE 3, a plasma membrane-associated scaffold protein involved in early brassinosteroid signaling. *Plos Genetics* **2019**, *15*, doi:10.1371/journal.pgen.1007904.
14. Zhang, B.; Wang, X.; Zhao, Z.; Wang, R.; Huang, X.; Zhu, Y.; Yuan, L.; Wang, Y.; Xu, X.; Burlingame, A.L.; et al. OsBRI1 Activates BR Signaling by Preventing Binding between the TPR and Kinase Domains of OsBSK3 via Phosphorylation. *Plant Physiology* **2015**, *170*, 1149-1161, doi:10.1104/pp.15.01668.
15. Li, Y.; Zhang, H.; Zhang, Y.; Liu, Y.; Li, Y.; Tian, H.; Guo, S.; Sun, M.; Qin, Z.; Dai, S. Genome-wide identification and expression analysis reveals spinach brassinosteroid-signaling kinase (BSK) gene family functions in temperature stress response. *Bmc Genomics* **2022**, *23*, doi:10.1186/s12864-022-08684-5.
16. Jia, Z.; Giehl, R.F.H.; Meyer, R.C.; Altmann, T.; von Wiren, N. Natural variation of BSK3 tunes brassinosteroid signaling to regulate root foraging under low nitrogen. *Nature Communications* **2019**, *10*, doi:10.1038/s41467-019-10331-9.
17. Neu, A.; Eilbert, E.; Asseck, L.Y.; Slane, D.; Henschen, A.; Wang, K.; Buergel, P.; Hildebrandt, M.; Musielak, T.J.; Kolb, M.; et al. Constitutive signaling activity of a receptor-associated protein links fertilization with embryonic patterning in Arabidopsis thaliana. *Proceedings of the National Academy of Sciences of the United States of America* **2019**, *116*, 5795-5804, doi:10.1073/pnas.1815866116.

 doi:10.20944/preprints202604.0627.v1

18. Shiu, S.H.; Karlowski, W.M.; Pan, R.S.; Tzeng, Y.H.; Mayer, K.F.X.; Li, W.H. Comparative analysis of the receptor-like kinase family in Arabidopsis and rice. *Plant Cell* **2004**, *16*, 1220-1234, doi:10.1105/tpc.020834.
19. Gao, C.; Zhao, Y.; Wang, W.; Zhang, B.; Huang, X.; Wang, Y.; Tang, D. BRASSINOSTEROID-SIGNALING KINASE 1 modulates OPEN STOMATA 1 phosphorylation and contributes to stomatal closure and plant immunity. *Plant Journal* **2024**, *120*, 45-59, doi:10.1111/tpj.16968.
20. Li, Q.; Shao, J.; Luo, M.; Chen, D.; Tang, D.; Shi, H. BRASSINOSTEROID-SIGNALING KINASE1 associates with and is required for cysteine protease RESPONSE TO DEHYDRATION 19-mediated disease resistance in Arabidopsis. *Plant Science* **2024**, *342*, doi:10.1016/j.plantsci.2024.112033.
21. Su, B.; Zhang, X.; Li, L.; Abbas, S.; Yu, M.; Cui, Y.; Baluska, F.; Hwang, I.; Shan, X.; Lin, J. Dynamic spatial reorganization of BSK1 complexes in the plasma membrane underpins signal-specific activation for growth and immunity. *Molecular Plant* **2021**, *14*, 588-603, doi:10.1016/j.molp.2021.01.019.
22. Chang, W.; Chen, L.; Xie, X.; Liu, M.; Song, D.; Yu, M.; Li, S.; Wei, L.; Qu, C.; Li, J.; et al. Construction of a FOX-hunting library to systematically identify functional genes and the salt-tolerant line isolation in Brassica napus. *Plant Physiology and Biochemistry* **2025**, *228*, doi:10.1016/j.plaphy.2025.110255.
23. Li, Z.-Y.; Xu, Z.-S.; He, G.-Y.; Yang, G.-X.; Chen, M.; Li, L.-C.; Ma, Y.-Z. A mutation in Arabidopsis BSK5 encoding a brassinosteroid-signaling kinase protein affects responses to salinity and abscisic acid. *Biochemical and Biophysical Research Communications* **2012**, *426*, 522-527, doi:10.1016/j.bbrc.2012.08.118.
24. Wang, J.; Shi, H.; Zhou, L.; Peng, C.; Liu, D.; Zhou, X.; Wu, W.; Yin, J.; Qin, H.; Ma, W.; et al. OsBSK1-2, an Orthologous of AtBSK1, Is Involved in Rice Immunity. *Frontiers in Plant Science* **2017**, *8*, doi:10.3389/fpls.2017.00908.
25. Yuan, H.; Xu, Z.; Chen, W.; Deng, C.; Liu, Y.; Yuan, M.; Gao, P.; Shi, H.; Tu, B.; Li, T.; et al. OsBSK2, a putative brassinosteroid-signalling kinase, positively controls grain size in rice. *Journal of Experimental Botany* **2022**, *73*, 5529-5542, doi:10.1093/jxb/erac222.
26. Li, S.; Xiang, X.; Diao, Z.; Xia, N.; Lu, L.; Zhang, J.; Chen, Z.; Tang, D. The OsBSK1-2-MAPK module regulates blast resistance in rice. *Crop Journal* **2024**, *12*, 110-120, doi:10.1016/j.cj.2023.11.009.
27. Daniel Pantoja-Benavides, A.; Garces-Varon, G.; Restrepo-Diaz, H. Foliar cytokinins or brassinosteroids applications influence the rice plant acclimatization to combined heat stress. *Frontiers in Plant Science* **2022**, *13*, doi:10.3389/fpls.2022.983276.
28. Halaji, B.; Haghighi, M.; Kovacs, G.P.; Mirmazloum, I.; Szego, A. The Role of Brassinosteroids and Nano-Encapsulated Brassinosteroids in Capsicum Pepper Growth and Physiological Adaptations to High-Temperature Stress. *Horticulturae* **2024**, *10*, doi:10.3390/horticulturae10101062.
29. Lv, J.; Dong, T.; Zhang, Y.; Ku, Y.; Zheng, T.; Jia, H.; Fang, J. Metabolomic profiling of brassinolide and abscisic acid in response to high-temperature stress. *Plant Cell Reports* **2022**, *41*, 935-946, doi:10.1007/s00299-022-02829-2.
30. Sadura, I.; Janeczko, A. Brassinosteroids and the Tolerance of Cereals to Low and High Temperature Stress: Photosynthesis and the Physicochemical Properties of Cell Membranes. *International Journal of Molecular Sciences* **2022**, *23*, doi:10.3390/ijms23010342.
31. Chen, C.; Chen, H.; Zhang, Y.; Thomas, H.R.; Frank, M.H.; He, Y.; Xia, R. TBtools: An Integrative Toolkit Developed for Interactive Analyses of Big Biological Data. *Molecular Plant* **2020**, *13*, 1194-1202, doi:10.1016/j.molp.2020.06.009.
32. Wan, Z.; Luo, S.; Zhang, Z.; Liu, Z.; Qiao, Y.; Gao, X.; Yu, J.; Zhang, G. Identification and expression profile analysis of the SnRK2 gene family in cucumber. *Peerj* **2022**, *10*, doi:10.7717/peerj.13994.
33. Hurst, L.D. The Ka/Ks ratio:: diagnosing the form of sequence evolution. *Trends in Genetics* **2002**, *18*, 486-487, doi:10.1016/s0168-9525(02)02722-1.
34. Szklarczyk, D.; Kirsch, R.; Koutrouli, M.; Nastou, K.; Mehryary, F.; Hachilif, R.; Gable, A.L.; Fang, T.; Doncheva, N.T.; Pyysalo, S.; et al. The STRING database in 2023: protein-protein association networks and functional enrichment analyses for any sequenced genome of interest. *Nucleic Acids Research* **2023**, *51*, D638-D646, doi:10.1093/nar/gkac1000.
35. Doncheva, N.T.; Jensen, L.J.; Morris, J.H.; Holze, H.; Kirsch, R.; Nastou, K.C.; Cuesta-Astroz, Y.; Rattei, T.; Szklarczyk, D.; Mering, C.v.; et al. Cytoscape stringApp 2.0: Analysis and Visualization of Heterogeneous Biological Networks. *Journal of Proteome Research* **2023**, *22*, 637-646, doi:10.1021/acs.jproteome.2c00651.

 doi:10.20944/preprints202604.0627.v1

36. Liu, W.; Dai, Z.; Jia, J.; Li, X.; Zhu, H.; Kan, X.; Zhu, B. Comparative physiological and transcriptomic analyses identify computationally predicted key genes and regulatory pathways in non-heading Chinese cabbage under heat stress. *Bmc Plant Biology* **2025**, *25*, doi:10.1186/s12870-025-07120-6.
37. Li, H.-s. Principles and Techniques of Plant Physiological and Biochemical Experiments; Higher Education Press: Beijing, 2000.
38. Jiao, Y.; Wickett, N.J.; Ayyampalayam, S.; Chanderbali, A.S.; Landherr, L.; Ralph, P.E.; Tomsho, L.P.; Hu, Y.; Liang, H.; Soltis, P.S.; et al. Ancestral polyploidy in seed plants and angiosperms. *Nature* **2011**, *473*, 97-U113, doi:10.1038/nature09916.
39. Rensing, S.A. Gene duplication as a driver of plant morphogenetic evolution. *Current Opinion in Plant Biology* **2014**, *17*, 43-48, doi:10.1016/j.pbi.2013.11.002.
40. Van de Peer, Y.; Mizrachi, E.; Marchal, K. The evolutionary significance of polyploidy. *Nature Reviews Genetics* **2017**, *18*, 411-424, doi:10.1038/nrg.2017.26.
41. Liu, L.; Xiang, Y.; Yan, J.; Di, P.; Li, J.; Sun, X.; Han, G.; Ni, L.; Jiang, M.; Yuan, J.; et al. BRASSINOSTEROID-SIGNALING KINASE 1 phosphorylating CALCIUM/CALMODULIN-DEPENDENT PROTEIN KINASE functions in drought tolerance in maize. *New Phytologist* **2021**, *231*, 695-712, doi:10.1111/nph.17403.
42. Shi, B.; Wang, Y.; Wang, L.; Zhu, S. Genome-Wide Identification of the Brassinosteroid Signal Kinase Gene Family and Its Profiling under Salinity Stress. *International Journal of Molecular Sciences* **2024**, *25*, doi:10.3390/ijms25158499.
43. Lee, H.J.; Lee, J.H.; Lee, S.G.; An, S.; Lee, H.S.; Choi, C.K.; Kim, S.K. Foliar application of biostimulants affects physiological responses and improves heat stress tolerance in Kimchi cabbage. *Horticulture Environment and Biotechnology* **2019**, *60*, 841-851, doi:10.1007/s13580-019-00193-x.
44. Neha; Twinkle; Mohapatra, S.; Sirhindi, G.; Dogra, V. Seed priming with brassinolides improves growth and reinforces antioxidative defenses under normal and heat stress conditions in seedlings of Brassica juncea. *Physiologia Plantarum* **2022**, *174*, doi:10.1111/ppl.13814.
45. Chen, Y.; Wang, Y.; Chen, H.; Xiang, J.; Zhang, Y.; Wang, Z.; Zhu, D.; Zhang, Y. Brassinosteroids Mediate Endogenous Phytohormone Metabolism to Alleviate High Temperature Injury at Panicle Initiation Stage in Rice. *Rice Science* **2023**, *30*, 70-86, doi:10.1016/j.rsci.2022.05.005.
46. Camejo, D.; Rodríguez, P.; Morales, A.; Dell'Amico, J.M.; Torrecillas, A.; Alarcón, J.J. High temperature effects on photosynthetic activity of two tomato cultivars with different heat susceptibility. *Journal of Plant Physiology* **2005**, *162*, 281-289, doi:10.1016/j.jplph.2004.07.014.
47. Ogweno, J.O.; Song, X.S.; Shi, K.; Hu, W.H.; Mao, W.H.; Zhou, Y.H.; Yu, J.Q.; Nogues, S. Brassinosteroids alleviate heat-induced inhibition of photosynthesis by increasing carboxylation efficiency and enhancing antioxidant systems in Lycopersicon esculentum. *Journal of Plant Growth Regulation* **2008**, *27*, 49-57, doi:10.1007/s00344-007-9030-7.
48. Tang, W.; Kim, T.-W.; Oses-Prieto, J.A.; Sun, Y.; Deng, Z.; Zhu, S.; Wang, R.; Burlingame, A.L.; Wang, Z.-Y. BSKs mediate signal transduction from the receptor kinase BRI1 in Arabidopsis. *Science* **2008**, *321*, 557-560, doi:10.1126/science.1156973.
49. Sreeramulu, S.; Mostizky, Y.; Sunitha, S.; Shani, E.; Nahum, H.; Salomon, D.; Ben Hayun, L.; Gruetter, C.; Rauh, D.; Ori, N.; et al. BSKs are partially redundant positive regulators of brassinosteroid signaling in Arabidopsis. *Plant Journal* **2013**, *74*, 905-919, doi:10.1111/tpj.12175.
50. Xia, H.; Ma, X.; Xu, K.; Wang, L.; Liu, H.; Chen, L.; Luo, L. Temporal transcriptomic differences between tolerant and susceptible genotypes contribute to rice drought tolerance. *Bmc Genomics* **2020**, *21*, doi:10.1186/s12864-020-07193-7.